Reactions of 1-Naphthyl Radicals with Ethylene. Single Pulse Shock Tube Experiments, Quantum Chemical, Transition State Theory, and Multiwell Calculations

Assa Lifshitz,* Carmen Tamburu, and Faina Dubnikova

Department of Physical Chemistry, The Hebrew University of Jerusalem, Jerusalem 91904, Israel

Received: September 11, 2007; In Final Form: November 6, 2007

The reactions of 1-naphthyl radicals with ethylene were studied behind reflected shock waves in a single pulse shock tube, covering the temperature range 950−1200 K at overall densities behind the reflected shocks of $\sim 2.5 \times 10^{-5}$ mol/cm^3. 1-Iodonaphthalene served as the source for 1-naphthyl radicals as its C−I bond dissociation energy is relatively small. It is only ∼65 kcal/mol as compared to the C−H bond strength in naphthalene which is ∼112 kcal/mol and can thus produce naphthyl radicals at rather low reflected shock temperatures. The [ethylene]/[1-iodo-naphthalene] ratio in all of the experiments was ∼100 in order to channel the free radicals into reactions with ethylene rather than iodonaphthalene. Four products resulting from the reactions of 1-naphthyl radicals with ethylene were found in the post shock samples. They were vinyl naphthalene, acenaphthene, acenaphthylene, and naphthalene. Some low molecular weight aliphatic products at rather low concentrations, resulting from the attack of various free radicals on ethylene were also found in the shocked samples. In view of the relatively low temperatures employed in the present experiments, the unimolecular decomposition rate of ethylene is negligible. Three potential energy surfaces describing the production of vinyl naphthalene, acenaphthene, and acenaphthylene were calculated using quantum chemical methods and rate constants for the elementary steps on the surfaces were calculated using transition state theory. Naphthalene is not part of the reactions on the surfaces. Acenaphthylene is obtained only from acenaphthene. A kinetics scheme containing 27 elementary steps most of which were obtained from the potential energy surfaces was constructed and computer modeling was performed. An excellent agreement between the experimental yields of the four major products and the calculated yields was obtained.

I. Introduction

The reaction of aryl radicals with unsaturated aliphatic hydrocarbons is one of the reaction channels that lead to the production of polycyclic aromatic hydrocarbons (PAH). This is particularly true when acetylene and its derivatives are concerned.[1−12] The same holds for the unsaturated aliphatic hydrocarbon radicals reacting with the aromatic compounds. While reactions with acetylene have been studied quite extensively,[1−8] reactions of aryl radicals with ethylene or of vinyl radicals with the aromatic compounds[9−12] are hardly mentioned in literature. When naphthyl radicals are concerned, their attack on ethylene, acetylene, and other unsaturated aliphatics can lead to both cyclization and a simple attachment. The same behavior is seen when $CH_2{=}CH^{\bullet}$, for example, attack naphthalene.[9] The relative rates of these two types of processes affect to some extent, among others, the rate of the PAH growth.

In this article we present experimental single pulse shock tube data of product formation and quantum chemical calculations in the system of 1-naphthyl radicals and ethylene where the 1-naphthyl radicals are obtained from the dissociation of 1-iodonaphthatene. We also compose a kinetics scheme and perform computer modeling based on the reaction pathways and the elementary steps on the calculated surfaces and compare the results of the calculations to the single pulse shock tube results.

* To whom correspondence should be addressed. E-mail: Assa@vms.huji.ac.il.

II. Experimental Section

1. Apparatus. The reactions of 1-naphthyl radicals with ethylene were studied behind reflected shock waves in a pressurized driver, 52-mm i.d., single-pulse shock tube. The shock tube had a 4-m driven section divided in the middle by a 52-mm i.d. ball valve. The driver section had a variable length up to a maximum of 2.7 m and could be varied in small steps in order to obtain the best cooling conditions. A 36-L dump tank was connected to the driven section at 45° angle toward the driver near the diaphragm holder in order to prevent reflection of transmitted shocks and in order to reduce the final driver gas pressure in the tube. The driven section was separated from the driver by "Mylar" polyester films of various thicknesses depending upon the desired shock strength.

The shock tube, the reaction mixture storage bulbs, the gas handling manifold, and the transfer tubes were all maintained at 170 ± 2 °C with a heating system containing 15 independent computer controlled heating elements. Reaction dwell times behind the reflected waves were approximately 2.0 ± 0.1 ms and cooling rates were $\sim 5 \times 10^5$ K/s.

Prior to performing an experiment, the tube and its gas handling system were pumped down to $\sim 3 \times 10^{-5}$ Torr. The reaction mixtures were introduced into the driven section between the ball valve and the end plate, and pure argon into the section between the diaphragm and the valve, including the dump tank. After each experiment, two gas samples were taken for analysis. One sample was transferred from the tube through a heated injection system to a Hewlett-Packard model 5890A gas chromatograph operating with a flame ionization detector

10.1021/jp077289s CCC: $40.75
Published on Web 01/12/2008

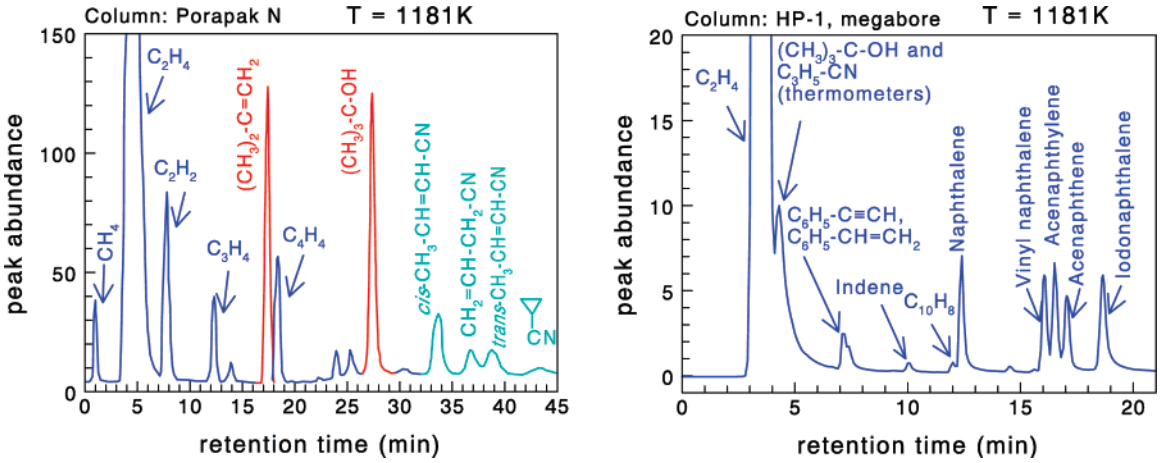

Figure 1. Typical chromatograms of a reaction mixture containing 0.05% 1-iodonaphthalene, 5% ethylene and 0.01% of each of the two chemical thermometers, shock-heated to 1181 K. The chromatogram on the left shows the low molecular weight aliphatic hydrocarbons, coming from the decomposition of ethylene. The peaks shown in red belong to the chemical thermometer: $(CH_3)_3C-OH \rightarrow (CH_3)_2C=CH_2 + H_2O$, and the ones in cyan to the thermometer: cyclopropanecarbonitrile → *c*-$CH_3CH=CHCN$, *t*-$CH_3CH=CHCN$ and $CH_2=CHCH_2CN$. The chromatogram on the right shows the high molecular weight aromatics that are coming from the reactions of naphthyl radicals with ethylene.

(FID), using a 15 m × 0.53 mm HP-1 megabore column, coated with methyl silicon gum. This analysis provided the concentrations of the heavy aromatics. The second sample, which gave the conversion of the chemical thermometers and the concentration of the low molecular weight ethylene decomposition products, was transferred from the shock tube via 100 cm^3 glass bulbs to a Carlo-Erba Vega series 2, model 6300 gas chromatograph using a 2 m Porapak-N column with a flame ionization detector.

2. Temperature Determination. Reflected shock temperatures were determined from the conversion of two standard reactions, the reactants of which were added in small quantities (0.01%) to the reaction mixtures to serve as chemical thermometers. Over the temperature range 950−1050 K, the reflected shock temperatures were determined from the extent of the total isomerization of cyclopropanecarbonitrile to *cis*- and *trans*-crotonitrile and 3-butenonitrile,[13] and over the temperature range 1050−1200 K, from the extent of decomposition of *tert*-butanol to isopropene and water:[14]

1. Cyclopropanecarbonitrile → *c*-$CH_3CH=CHCN$, *t*-$CH_3CH=CHCN$, and $CH_2=CHCH_2CN$, $k_{uni} = 3.2 \times 10^{14} \exp(-57840/RT)\ s^{-1}$,

2. $(CH_3)_3C-OH \rightarrow (CH_3)_2C=CH_2 + H_2O$, $k_{uni} = 8.5 \times 10^{13} \exp(-63120/RT)\ s^{-1}$,

where R is expressed in units of cal/mol.

Reflected shock temperatures T_5 were calculated from the relation

$$T_5 = -(E/R)/\left[\ln\left\{-\frac{1}{At}\ln(1-\chi)\right\}\right]$$

where t is the reaction dwell time, A and E are the preexponential factors and the activation energies of the standard reactions, and χ is the extent of reaction defined as

$$\chi = [\text{reactant}]_t/([\text{reactant}]_t + [\text{product(s)}]_t)$$

Density ratios were calculated from the measured incident shock velocities using the three conservation equations and the ideal gas equation of state.

3. Materials and Analysis. Reaction mixtures containing 0.05% iodonaphthalene, 5% ethylene, and 0.01% of each one of the two chemical thermometers diluted in argon were prepared in 12 L glass bulbs and stored at 170 ± 2 °C and 700 Torr. Both the bulbs and the line were pumped down to approximately 3 × 10^{-5} Torr before the preparation of the mixtures. 1-Iodonaphthalene served as the source of naphthyl radicals as the C−I bond dissociation energy in 1-iodonaphthalene is by some 46 kcal/mol smaller than that of the C−H bond in naphthalene (66 vs.112) and can thus produce naphthyl radicals at much lower temperatures.[15] The reason for the high [ethylene]/[1-iodonaphthalene] ratio, (∼100), comes to channel all the radicals, particularly the naphthyl radicals to reactions with ethylene rather than 1-iodonaphthalene.

1-Iodonaphthalene was obtained from Aldrich Chemical Co. and had a purity of ∼97%. None of the four major products, acenaphthene, vinyl naphthalene, naphthalene, and acenaphthylene, were found in the unshocked samples. The argon used was Matheson ultrahigh purity grade, listed as 99.9995%, and the helium driver gas was Matheson pure grade, listed as 99.999%. All materials were used without further purification.

Typical chromatograms of a reaction mixture containing 0.05% iodonaphthalene, 5% ethylene and 0.01% of each of the two chemical thermometers shock-heated to 1181 K are shown in Figure 1. As can be seen naphthyl acetylene is not among the reaction products.

4. Data Reduction. The concentrations of 1-iodonaphthalene and the four, two ring aromatic products in the shocked samples $C_5(\text{pr}_i)$ were calculated from their GC peak areas using the following set of relations that are based on two fused aromatic ring balance

$$C_5(\text{pr}_i) = A(\text{pr}_i)/S(\text{pr}_i) \times \{C_5(\text{reactant})_0/A(\text{reactant})_0\} \quad \text{(I)}$$

where

$$C_5(\text{reactant})_0 = \{p_1 \times \%(\text{reactant}) \times \rho_5/\rho_1\}/100RT_1 \quad \text{(II)}$$

and

$$A(\text{reactant})_0 = A(\text{reactant})_t + \Sigma A(\text{pr}_i)_t/S(\text{pr}_i) \quad \text{(III)}$$

$C_5(\text{reactant})_0$ is the concentration of 1-iodonaphthalene behind the reflected shock prior to reaction and $A(\text{reactant})_0$ is its calculated GC peak area prior to reaction (eq III) where: $A(\text{pr}_i)_t$ is the peak area of a product i in the shocked sample, and $S(\text{pr}_i)$ is its sensitivity relative to that of the reactant, ρ_5/ρ_1 is the

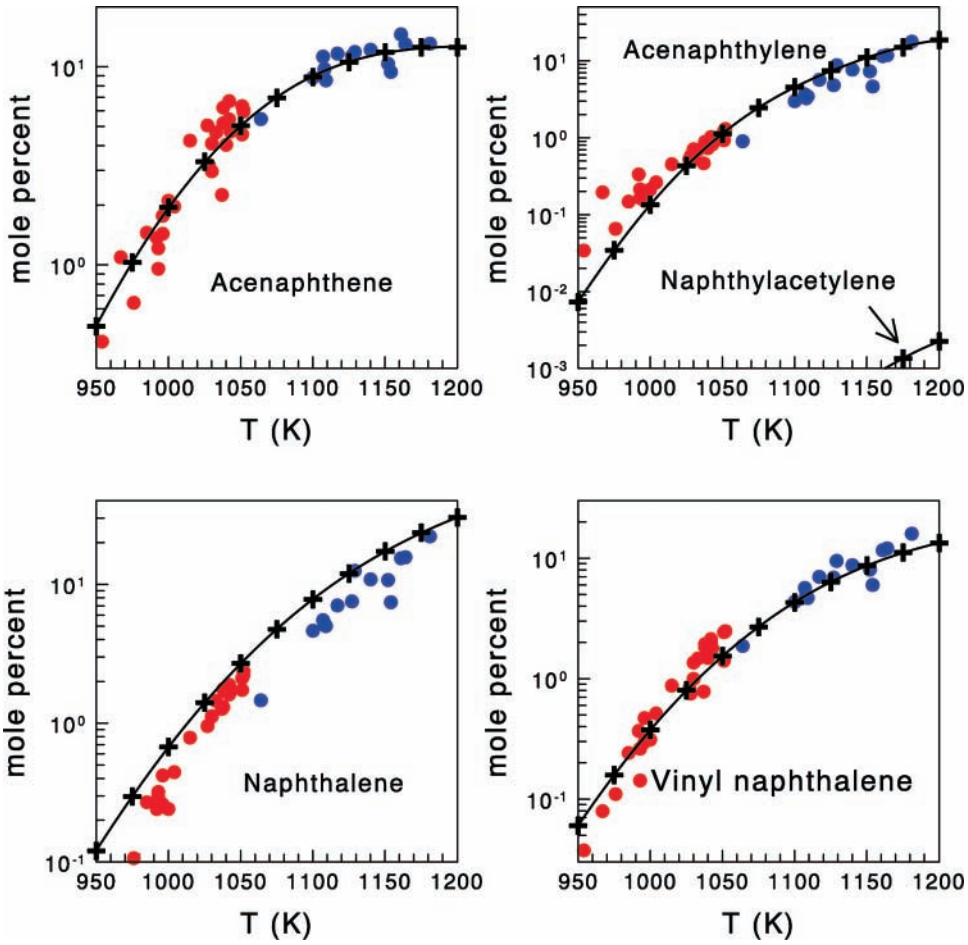

Figure 2. Yields of the four major products are shown as mole percent vs temperature on a semilog scale. The reflected shock temperatures of the points shown in red, were calculated using the extent of the total isomerization of cyclopropane carbonitrile and the ones in blue from the extent of decomposition of tert.-butyl alcohol. The black points (+) are the calculated yields and the lines are the best fit to these points.

compression behind the reflected shock, and T_1 is the initial temperature, 443 K in the present series of experiments.

The low molecular weight aliphatic products that are coming from ethylene and the very low concentrations of some single ring aromatics such as phenyl acetylene and indene were not taken into account in these calculations. Only naphthalene, acenaphthene, vinyl naphthalene and acenaphthylene were considered.

The G.C. sensitivities of the products relative to the reactant were determined from standard mixtures. GC peak areas were recorded and evaluated using the "Chromatography Station for Windows-CSW 1.7" software, produced by: Data Apex Ltd. 1998, The Czech Republic. They were transferred after each analysis to a PC for data reduction and graphical presentation.

III. Experimental Results

Some 45 tests were run with reaction mixtures containing 0.05% 1-iodonaphthalene, 5% ethylene, and the two chemical thermometers diluted in argon, covering the temperature range 950−1200 K. Densities behind the reflected shocks were ~2.5 × 10^{-5} mol/cm^3 corresponding to p_5 = ~1400−1850 Torr depending upon the temperature. Four major products resulting from the reactions of the system containing 1-iodonaphthalene and ethylene, namely, acenaphthene, vinyl naphthalene, acenaphthylene, and naphthalene, were found in the shocked samples. Figure 2 shows the actual data points of the four above mentioned products as product yield vs temperature, and Figure 3 shows the overall decomposition of 1-iodo-naphthalene. The

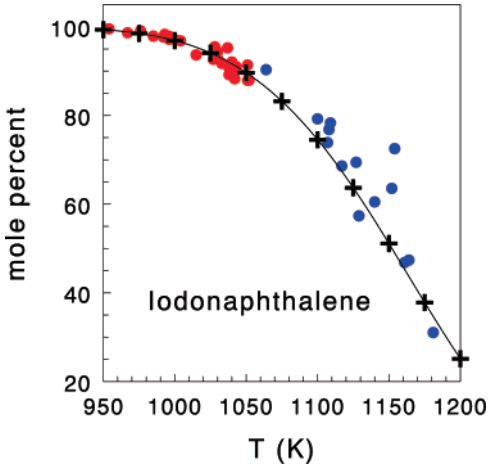

Figure 3. Total decomposition of 1-iodonaphthalene.

reflected shock temperatures of the low-temperature data points (shown in red) were calculated from the isomerization rate of *c*-C_3H_5CN and the high-temperature data (shown in blue) were calculated from the extent of decomposition of tertiary butanol. The + sign on the lines are the calculated points and the lines are the best fits to these points. Many rate constants in the scheme where evaluated by quantum chemical calculations as will be described later.

IV. Quantum Chemical and Rate Constant Calculations

1. Quantum Chemical Calculations. We used the Becke three-parameter hybrid method[16] with Lee−Yang−Parr cor-

relation functional approximation with unrestricted open shell wavefunctions (uB3LYP)[17] and the Dunning correlation consistent polarized valence double ζ(cc-pVDZ) basis set.[18] Structure optimization of the reactants and products was done using the Berny geometry optimization algorithm.[19] For determining transition state structures, we used the combined synchronous transit-guided quasi-Newton (STQN) method.[20] Higher level (CI) calculations were done using these structures.

All of the calculations were performed without symmetry restrictions. Vibrational analyses were done at the same level of theory to characterize the optimized structures as local minima or transition states. Calculated vibrational frequencies and entropies (at uB3LYP level) were used to evaluate preexponential factors of the reactions under consideration. All of the calculated frequencies, the zero-point energies, and the thermal energies are of harmonic oscillators. The calculations of the intrinsic reaction coordinate (IRC), to check whether the transition states under consideration connect the expected reactants and products, were done at the B3LYP level of theory with the same basis set as was used for the stationary point optimization. These calculations were done on all of the transition states.

Each optimized uB3LYP structure was recalculated at a single-point coupled cluster, including both single and double substitutions with triple excitations uCCSD(T). The uCCSD-(T) calculations were performed with the frozen core approximation. All of the reported relative energies include zero-point energy correction (ZPE). The DFT and CCSD(T) computations were carried out using the Gaussian 03 program package.[21]

2. Rate Constant Calculations. In order to evaluate first-order rate constants from the quantum chemical calculations the relation

$$k_{\infty} = \Gamma(T)\sigma(kT/h)\exp(\Delta S^{\#}/R)\exp(-\Delta H^{\#}/RT) \qquad (1)$$

was used,[22,23] where h is Planck constant, k is Boltzmann factor, σ is the degeneracy of the reaction coordinate, $\Delta H^{\#}$ and $\Delta S^{\#}$ are the temperature-dependent enthalpy and entropy of activation respectively and $\Gamma(T)$ is the tunneling correction. For the unimolecular reactions, $\Delta H^{\#} = \Delta E^{\#}$, where $\Delta E^{\#}$ is the energy difference between the transition state and the reactant. $\Delta E^{\#}$ is equal to $\Delta E^{0}_{\text{total}} + \Delta E_{\text{thermal}}$ where $\Delta E^{0}_{\text{total}}$ is obtained by taking the difference between the total energies of the transition state and the reactant and $\Delta E_{\text{thermal}}$ is the difference between the thermal energies of these species.

The tunneling effect, $\Gamma(T)$, was estimated using Wigner's inverted harmonic model,[24] where

$$\Gamma(T) = 1 + \frac{1}{24} \times \left(\frac{hc\bar{\lambda}^{\#}}{kT}\right)^2$$

and $\bar{\lambda}^{\#}$ is the imaginary frequency of the reaction coordinate in cm^{-1}.[25,26] The correction was significant only for high $\bar{\lambda}^{\#}$.

Among the fifteen rate constants that were calculated by quantum chemical methods and where introduced into overall kinetics scheme (Table 3), nine were unimolecular and six were bimolecular. For the latter, only the barriers were calculated and the pre-exponential factors were estimated on the basis of similar reactions, the rate constants of which are available in the literature.[14] In view of relatively low temperatures covered in this investigation and the high size molecules involved, RRKM calculations were not done.

TABLE 1: Zero-Point Energies, Relative Energies ΔE,[a] Imaginary Frequencies,[b] and Entropies[c] of the Species on the Three Potential Energy Surfaces

	uB3LYP			uCCSD(T)
species	ZPE	S^c	ν^b	ΔE^a
Potential Energy Surface A				
1-naphthyl + C_2H_4	116.09			34.99
TS1	116.74	103.67	(i-209)	37.51
INT(R1)•	**118.20**	**98.61**		**0.0**
TS2	113.77	98.38	(i-682)	35.01
1-vinylnaphthalene + H•	113.01			29.07
TS3	118.23	91.38	(i-581)	21.23
INT(R2)•	120.03	91.12		−9.76
TS4	115.33	91.95	(i-688)	19.71
acenaphthene + H•	114.16			13.48
Potential Energy Surface B				
1-naphthyl + C_2H_4	116.09			34.99
TS5	113.21	105.85	(i-1518)	43.21
naphthalene + C_2H_3•	115.16			32.48
TS6	116.02	102.09	(i-353)	39.52
INT(R3)•	118.55	98.71		5.67
TS7	114.05	97.09	(i-838)	37.10
1-vinylnaphthalene + H•	113.01			29.07
TS8	115.36	95.37	(i-1698)	46.57
INT(R1)•	**118.20**	**98.61**		**0.0**
Potential Energy Surface C				
acenaphthene + H•	114.16			0.0
TS9	112.90	93.23	(i-782)	6.39
INT(R4)• + H_2	111.91			−13.65
TS10 + H_2	100.12	91.95	(i-335)	27.29
acenaphthylene + H• + H_2	99.9			24.75

[a] Relative energies in kcal/mol. $\Delta E = \Delta E_{\text{total}} + \Delta(\text{ZPE})$. [b] Imaginary frequency in cm^{-1}. [c] Entropies at 298 K in cal/(K mol).

V. Results of the Quantum Chemical Calculations

Two potential energy surfaces leading to the formation of 1-vinyl naphthalene and acenaphthene and one surface that describe the formation of acenaphthylene from the product acenaphthene were calculated. The first two surfaces begin with a reaction between 1-naphthyl radicals and ethylene where the source of 1-naphthyl radicals is the decomposition of 1-iodonaphthalene. The first step in surface (A) involves an electrophilic attachment of 1-naphthyl radical to ethylene and in surface (B) the first step is an abstraction of a hydrogen atom from ethylene producing naphthalene and C_2H_3•. Surface (C) begins with an abstraction of a hydrogen atom from acenaphthene toward to formation of acenaphthylene.

1. Potential Energy Surface A: 1-Naphthyl• + C_2H_4 → $C_{10}H_7-CH_2-CH_2$• and so on... The potential energy surface A is shown in Figure 4. The energetics and other parameters relevant to this surface are shown in Table 1A. The electrophilic addition process has a very low barrier of ∼2.5 kcal/mol (TS1) toward the formation of a rather stable 1-naphthyl ethyl radical (INT(R1)) where its energy is taken as zero in both the figure and in the table. There are two reaction channels starting from INT(R1). One channel leads to the formation of acenaphthene and the second channel leads to the formation of vinyl naphthalene, both involve H-atom ejection. In the radical INT-(R1) there is practically a free rotation around the $CH_2-C<$ bond (a barrier of 0.62 kcal/mol). The energy barrier for the isomerization INT(R1) → INT(R2) via transition state TS3 is thus due only to the bend of the CH_2•$-CH_2-C<$ group rather then its rotation process. This strong bending toward the ring closure introduces considerable stiffness to the transition state TS3 that is apparently a late transition state. The low pre-exponential factor for the INT(R1) → INT(R2) isomerization (Table 1) is due to the large negative difference in the entropy between the two above mentioned intermediates (−9.64 cal/

TABLE 2: Calculated Thermodynamic Properties of Radical Intermediates at 298 K[a]

Specie	Structure	$\Delta_f H^o$	S^o
INT(R1)•	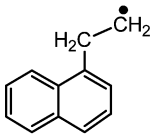	74.4	98.6
INT(R2)•	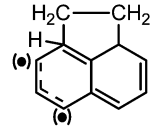	64.7	91.1
INT(R3)•	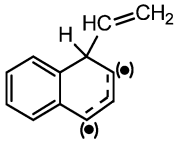	80.1	98.7
INT(R4)•	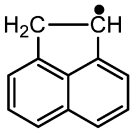	75.8	89.0
INT(R5)•	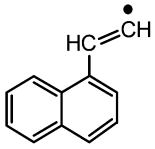	115.7	95.3
INT(R6)•	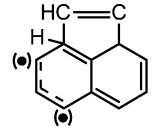	95.0	89.2

[a] $\Delta_f H°$ in kcal/mol and entropies in cal/(K mol). The symbol (•) denotes partial free electron density.

K.mol). The barrier of the rate determining step, for the formation of acenaphthene namely, INT(R2) → acenaphthene + H•, = ∼29.5 kcal/mol (TS4), is smaller than that for the formation of vinyl naphthalene which is ∼35 kcal/mol (TS2).

Similar processes with the benzene ring have been reported in the literature.[9−12] The electrophilic addition of phenyl radical to ethylene was calculated using CBS-QB3/B3LYP//6-311++G-(d,p) level of theory[9] to have a barrier of 2.3 kcal/mol, that is very similar to the barrier of the equivalent reaction with naphthyl radicals. Also, the ejection of a hydrogen atom from phenyl ethyl radical has a barrier of 35.1 kcal/mol,[9] which is practically identical to the barrier for H-atom ejection from 1-naphthyl ethyl radical (INT(R1) via transition state TS2) to form vinyl naphthalene.

2. Potential Energy Surface B: 1-Naphthyl• + C_2H_4 → Naphthalene + C_2H_3• and so on... The reaction channels that appear on this surface lead also to the formation of both vinyl naphthalene and acenaphthene. The surface is shown in Figure 5. The energetics and other parameters relevant to this surface are shown in Table 1B. The surface begins with an abstraction of a hydrogen atom from ethylene by naphthyl radical with a barrier of ∼8.2 kcal/mol via transition state TS5 forming naphthalene and C_2H_3•. It is followed by an attachment of the C_2H_3• to naphthalene forming a rather stable intermediate INT-(R3) with a barrier of ∼7 kcal/mol (TS6). The free electron density in this radical is distributed between two carbon atoms in the ring. The intermediate INT(R3) has now two reaction channels. One channel forms INT(R1), where the latter is a starting point for the production of both vinyl naphthalene and acenaphthene (see Figure 4). This channel, however, does not contribute much to the formation of these two products. This is the result of the high barrier of ∼39 kcal/mol. The second channel produces 1-vinyl naphthalene via transition state TS7 with the ejection of a hydrogen atom. The barrier is ∼31.5 kcal/mol.

The equivalent reaction of naphthalene + C_2H_3• → INT(R3) in benzene was calculated to have a barrier of ∼9 kcal/mol,[9] very similar to value calculated in this study.

3. Potential Energy Surface C: Production of Acenaphthylene from Acenaphthene. The production of acenaphthylene from acenaphthene involves the removal of two hydrogen atoms from acenaphthene. The surface is shown in Figure 6. The energetics and other parameters relevant to this surface are shown in Table 1(C). The process proceeds in two steps where the first one is an abstraction of a hydrogen atom from acenaphthene and the second step is an ejection of a hydrogen atom from the radical INT(R4). When the abstraction is by H-atom as a radical, the barrier of the fist step is ∼6.4 kcal/mol (TS9) and the ejection of a hydrogen atom from INT(R4) requires ∼41 kcal/mol (TS10).

VI. Multiwell Calculations and Kinetics Modeling

1. Reaction Scheme and Results of the Computer Modeling. In order to evaluate the yields of the four major products: acenaphthene, vinyl naphthalene, naphthalene and acenaphthylene, a kinetics scheme was constructed and computer modeling was carried out. Table 2 provides a glossary of the radical intermediates that are part of the scheme and gives the calculated values of $\Delta_f H°$ and $S°$ of these species at 298 K. The values were obtained by quantum chemical calculations at the uCCSD-(T)//uB3LYP/cc-pVDZ level of theory and are based on the known values of the heat of formation of acenaphthene and acenaphthylene. The thermochemical values at different temperatures were used to calculate equilibrium and rate constants of the back reactions of the elementary steps on the potential energy surfaces.

The kinetics scheme is shown in Table 3, and it contains three categories of reactions. One category contains all of the unimolecular steps that appear on the three potential energy surfaces for which both the barriers and the pre-exponential factors were calculated by quantum chemical methods (9 reactions). The second category contains all of the bimolecular reactions on the surfaces for which only the barriers were calculated but the pre-exponential factors were estimated on the basis of known similar chemical reactions (6 reactions).[14] These two categories of reactions are printed in bold letters in Table 3, where the first category is marked with a in the reference column and the second category is marked with b. The third category of reactions (reactions 1−11 and 21) contains elementary steps that are part of the scheme, but not of the potential energy surfaces. Their rate constants were taken from the literature or were estimated.[14,27−30] The rate parameters for four reactions (reactions 24−27) that contribute to the production of acenaphthylene from acenaphthene were taken from a study on the reaction of 1-iodonaphthalene with acetylene that is now being prepared for publication.[31]

The rate constants of the unimolecular steps on the surfaces were evaluated by the quantum chemical calculations at several

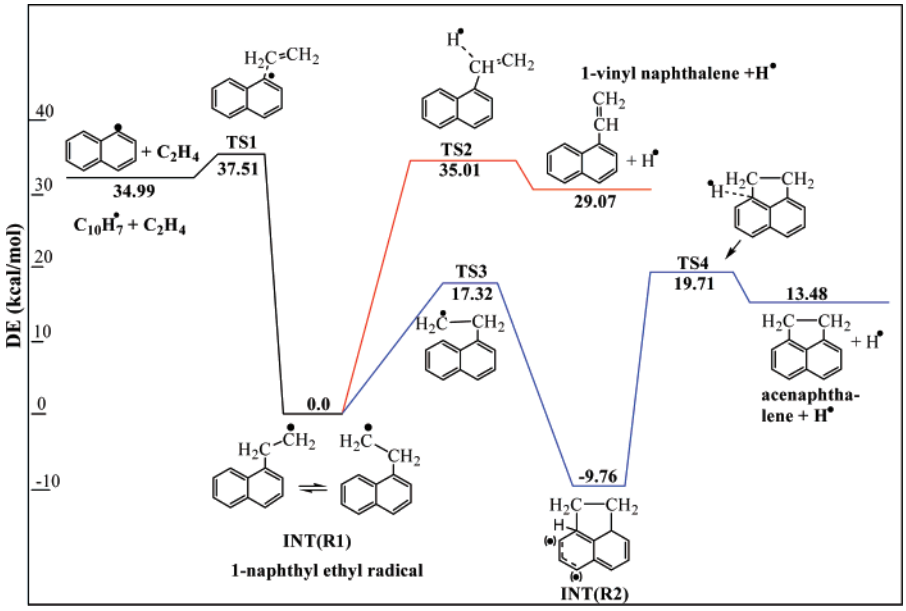

Figure 4. Potential energy surface 1(A) based on the initiation reaction: $1\text{-}C_{10}H_7^{\bullet} + C_2H_4 \rightarrow C_{10}H_7{-}CH_2{-}CH_2^{\bullet}$. The surface has two reaction channels, one producing vinyl naphthalene and the other producing acenaphthene.

TABLE 3: Kinetics Scheme for the 1-Iodonaphthalene−Ethylene Reaction System

no.	reactions	A	E	k_f (1050 K)	k_r (1050 K)	ΔS_r (1050 K)	ΔH_r (1050 K)	ref
1	iodonaphthalene → naphthyl• + I•	8.59×10^{14}	65.2	23.1	9.95×10^{12}	30.9	64.6	27
2	$C_2H_4 + Ar \rightarrow C_2H_3^{\bullet} + H^{\bullet} + Ar$	3.39×10^{17}	97.3	1.92×10^{-3}	1.51×10^{17}	35.3	109	14
3	$C_2H_4 + H^{\bullet} \rightarrow C_2H_3^{\bullet} + H_2$	$1.33 \times 10^6 T^{2.53}$	12.2	1.66×10^{11}	9.72×10^9	8.07	2.55	14
4	$C_2H_3^{\bullet} \rightarrow C_2H_2 + H^{\bullet}$	2.37×10^{14}	30.7	9.67×10^7	3.19×10^{16}	23.6	42.0	14
5	$C_2H_3^{\bullet} + C_2H_4 \rightarrow C_4H_6 + H^{\bullet}$	5.37×10^{11}	7.3	1.51×10^{10}	1.66×10^{-1}	52.0	1.93	28
6	$H^{\bullet} + H^{\bullet} + Ar \rightarrow H_2 + Ar$	$8.11 \times 10^{17} T^{-0.81}$	0.160	2.76×10^{15}	2.05×10^{-6}	−27.2	−106	14
7	iodonaphthalene + H• → naphthyl• + HI	2.00×10^{14}	11.0	1.03×10^{12}	6.87×10^8	6.31	−8.63	est
8	iodonaphthalene + H• → naphthalene + I•	1.00×10^{14}	13.0	1.97×10^{11}	58.9	−2.85	−48.8	est
9	H• + I• + Ar → HI + Ar	$2.00 \times 10^{21} T^{-1.87}$	0	4.48×10^{15}	6.96	−24.6	−73.2	29 est
10	$C_2H_3^{\bullet} + I^{\bullet} \rightarrow C_2H_3I$	4.40×10^{12}	1.0	2.72×10^{12}	7.78	−28.8	−62.0	est
11	naphthalene → naphthyl• + H•	5.01×10^{15}	108	1.75×10^{-7}	2.52×10^{14}	33.7	113	30
12	**naphthyl• + C_2H_4 → INT(R1)•**	$\mathbf{3.00 \times 10^{12}}$	**2.52**	$\mathbf{8.97 \times 10^{11}}$	$\mathbf{7.54 \times 10^7}$	**−34.1**	**−31.7**	***b***
13	**INT(R1)• → vinylnaphthalene + H•**	$\mathbf{1.33 \times 10^{14}}$	**37.3**	$\mathbf{2.27 \times 10^6}$	$\mathbf{1.02 \times 10^{12}}$	**24.4**	**29.0**	***a***
14	**INT(R1)• → INT(R2)•**	$\mathbf{4.16 \times 10^{11}}$	**22.0**	$\mathbf{1.10 \times 10^7}$	$\mathbf{8.00 \times 10^6}$	**−9.64**	**−10.8**	***a***
15	**INT(R2)• → acenaphthene + H•**	$\mathbf{1.26 \times 10^{14}}$	**32.0**	$\mathbf{2.76 \times 10^7}$	$\mathbf{3.97 \times 10^{11}}$	**28.4**	**26.0**	***a***
16	**naphthyl• + C_2H_4 → naphthalene + C_2H_3•**	$\mathbf{3.00 \times 10^{12}}$	**10.6**	$\mathbf{1.90 \times 10^{10}}$	$\mathbf{1.04 \times 10^9}$	**1.57**	**−4.42**	***b***
17	**naphthalene + C_2H_3• → INT(R3)•**	$\mathbf{3.00 \times 10^{12}}$	**7.03**	$\mathbf{1.03 \times 10^{11}}$	$\mathbf{2.53 \times 10^9}$	**−35.9**	**−21.7**	***b***
18	**INT(R3)• → vinylnaphthalene + H•**	$\mathbf{3.46 \times 10^{13}}$	**33.7**	$\mathbf{3.29 \times 10^6}$	$\mathbf{9.27 \times 10^{10}}$	**24.6**	**23.5**	***a***
19	**INT(R3)• → INT(R1)•**	$\mathbf{7.91 \times 10^{12}}$	**42.3**	$\mathbf{1.27 \times 10^4}$	$\mathbf{7.99 \times 10^2}$	**0.247**	**−5.52**	***a***
20	**acenaphthene + H• → INT(R4)•** + H_2	$\mathbf{1.00 \times 10^{14}}$	**6.39**	$\mathbf{4.68 \times 10^{12}}$	$\mathbf{9.58 \times 10^8}$	**4.0**	**−13.5**	***b***
21	acenaphthene + C_2H_3• → INT(R4)• + C_2H_4	3.00×10^{13}	8.0	6.49×10^{11}	2.27×10^9	−4.07	−16.1	est
22	**INT(R4)• → acenaphthylene + H•**	$\mathbf{7.96 \times 10^{14}}$	**44.1**	$\mathbf{5.23 \times 10^5}$	$\mathbf{9.65 \times 10^{12}}$	**27.9**	**40.5**	***a***
23	**naphthyl• + H_2 → naphthalene + H•**	$\mathbf{4.00 \times 10^{12}}$	**7.90**	$\mathbf{9.13 \times 10^{10}}$	$\mathbf{8.52 \times 10^{10}}$	**−6.50**	**−6.97**	***b***
24	**naphthyl• + C_2H_2 → INT(R5)•**	$\mathbf{3.00 \times 10^{12}}$	**4.43**	$\mathbf{3.59 \times 10^{11}}$	$\mathbf{2.00 \times 10^7}$	**−35.3**	**−33.8**	***b***
25	**INT(R5)• → naphthylacetylene + H•**	$\mathbf{6.20 \times 10^{12}}$	**41.2**	$\mathbf{1.67 \times 10^4}$	$\mathbf{4.08 \times 10^8}$	**30.7**	**29.6**	***a***
26	**INT(R5)• → INT(R6)•**	$\mathbf{1.45 \times 10^{12}}$	**19.7**	$\mathbf{1.15 \times 10^8}$	$\mathbf{1.60 \times 10^5}$	**−7.14**	**−21.2**	***a***
27	**INT(R6)• → acenaphthylene + H•**	$\mathbf{1.22 \times 10^{14}}$	**30.4**	$\mathbf{5.83 \times 10^7}$	$\mathbf{1.30 \times 10^{11}}$	**27.3**	**21.1**	***a***

[a] Calculated. [b] Calculated barrier, estimated preexponent.

temperatures covering the temperature range 950−1200 K, over which the single pulse shock-tube experiments were carried out. These were then plotted as ln k vs $1/T$ to obtain Arrhenius type rate constants that were used in the modeling. The calculated Arrhenius activation energies and pre-exponential factors are somewhat different from barriers and the pre-exponential factors that were calculated on the surfaces.

It should be mentioned that the dissociation of naphthalene to naphthyl radical + H• contains both 1- and 2-napthyl. The latter can produce 2-vinylnaphthalene but no acenaphthene. We could not identify in the post-shock mixtures two isomers of vinyl naphthalene and suspected that they could not be separated on the GC. So both the calculations and the experiments contain the two isomers.

The results of the modeling are shown in Figures 2 and 3 as solid lines in comparison with the experimental yields. The + sign on the lines are the calculated points and the lines are the best fits to these points. As can be seen the agreement is excellent.

2. Sensitivity Analysis. We ran also several sensitivity tests. In one test reactions were eliminated from the scheme, one by one, by multiplying their rate constants by a factor of 1×10^{-10}, and in another test the rate constants were multiplied, one by one, by a factor of 3. Each test was run at two different

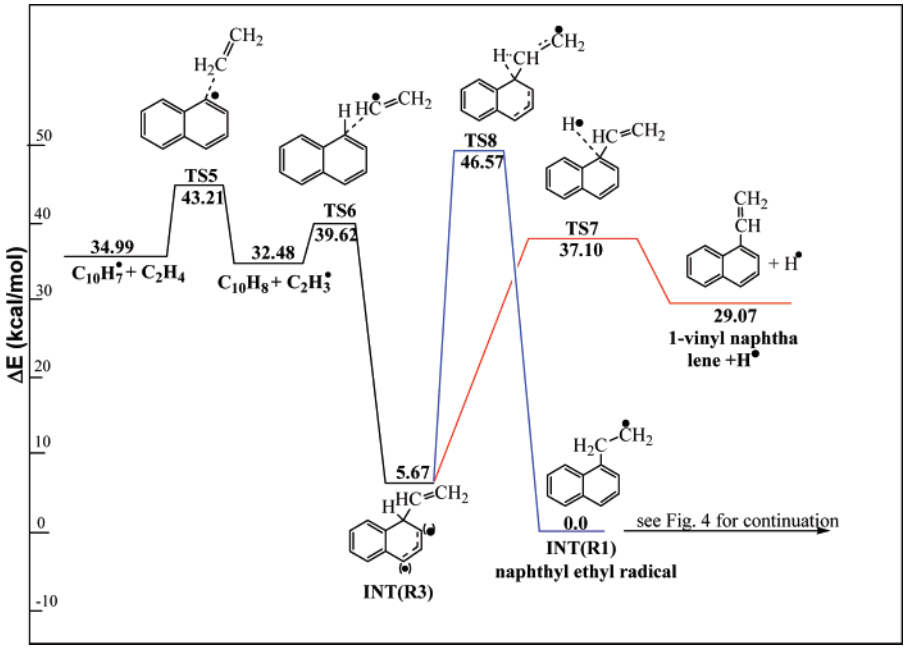

Figure 5. Potential energy surface 1(B) based on the initiation reaction: $1\text{-}C_{10}H_7^{\bullet} + C_2H_4 \rightarrow C_{10}H_8 + C_2H_3^{\bullet}$. The surface has two reaction channels, one leading to the production of acenaphthene and the other producing vinyl naphthalene. The contribution to the acenaphthene yield is negligible.

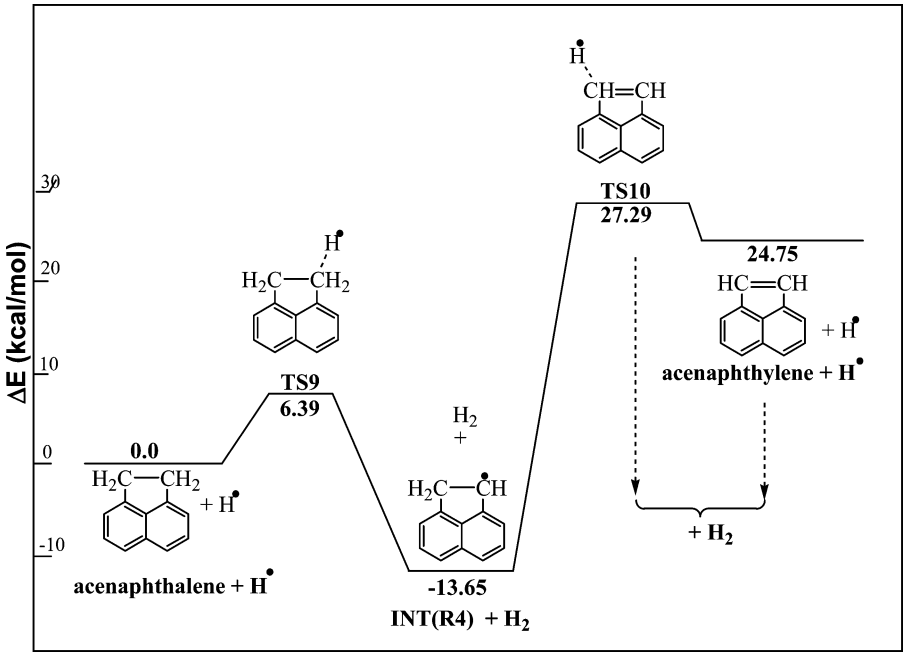

Figure 6. Potential energy surface 1(C) describes the production of acenaphthylene from acenaphthene. It has two steps: an abstraction of a hydrogen atom from acenaphthene followed by an ejection of another hydrogen atom.

temperatures: at the lower temperature end (950 K), and at the upper temperature end of the study (1175 K). The results of the tests are shown in Tables 4 and 5. They give the sensitivity spectrum of the four major products and for naphthyl radicals. Reactions with sensitivity factors of less than ±10% for all of the five products are not included in the tables.

There are 9 reactions that have no effect at all on the results of the product yields at both the low and the high temperatures, even when they are completely eliminated from the scheme (Table 4). These reactions are either side reactions such as the recombinations $H^{\bullet}+H^{\bullet}+Ar \rightarrow H_2$ or $H^{\bullet}+I^{\bullet}+Ar \rightarrow HI$ or reactions that are very slow such as, for example, the self-dissociation of ethylene. Another group of reactions are those that appear in parallel to other reactions that produce the same products at a much higher rate. Such reactions, for example, are reactions 18 and 19, (Table 3). When the rate constants are multiplied by a factor of 3 (Table 5), additional reactions join the group that has a very small effect.

Although most of the sensitivity factors that appear in Tables 4 and 5 are self-explanatory, there are some features that should be mentioned, in particular when a comparison is made between their values at high and at low temperature. In most of the reactions, the sensitivity factors at the low-temperature end are higher than those at the high-temperature end, in particular when the rate constant multiplication factor is 3 (Table 5). The self-dissociation of iodonaphthalene (Reaction 1), for example, has a very strong effect on the yields of all the four major products at 950 K owing to the initial production of naphthyl radicals. At 1075 K, its effect drops by almost an order of magnitude owing to the fact that at this temperature, most of the

TABLE 4: Sensitivity Factors (γ) in Percent for Elimination of Elementary Steps from the Kinetics Scheme[a]

no.	reactions	vinylnaphthalene	naphthalene	acenaphthene	acenaphthylene	naphthyl(R)
1	iodonaphthalene → naphthyl$^\bullet$ + I$^\bullet$	−99/−99	−99/−99	−100/−100	−99/−99	−99/−99
3	C_2H_4 + H$^\bullet$ → $C_2H_3^\bullet$ + H_2	31/8	40/61	30/−26	58/43	49/26
4	$C_2H_3^\bullet$ → C_2H_2 + H$^\bullet$	−69/65	−87/−19	−68/−19	−85/47	−72/78
7	iodonaphthalene + H$^\bullet$ → naphthyl$^\bullet$ + HI	−71/−24	−25 /−14	−71 /−22	−68/−18	−74/3
8	iodonaphthalene + H$^\bullet$ → naphthalene + I$^\bullet$	26/0	−51/−10	25/−6	80/12	32/1
10	$C_2H_3^\bullet$ + I$^\bullet$ → C_2H_3I	0/−14	0/10	0/−52	1/43	1/−19
11	naphthalene → naphthyl$^\bullet$ + H$^\bullet$	2/4	0/−17	2/−13	4/37	2/−8
12	naphthyl$^\bullet$ + C_2H_4 → INT(R1)$^\bullet$	−99/−99	326/102	−99 /−99	−71 /−54	955/ 178
13	INT(R1)$^\bullet$ → vinylnaphthalene + H$^\bullet$	−99/−99	3/14	11/28	10/20	8/21
14	INT(R1)$^\bullet$ → INT(R2)$^\bullet$	451/79	127/43	−99/−99	−85/−64	366/76
15	INT(R2)$^\bullet$ → acenaphthene + H$^\bullet$	447/79	125/43	−99/−99	−85/−64	365/76
16	naphthyl$^\bullet$ + C_2H_4 → naphthalene + $C_2H_3^\bullet$	7/26	−35/−44	7/29	7/19	7/26
20	acenaphthene + H$^\bullet$ → INT(R4)$^\bullet$ + H_2	0/0	0/0	1/49	−83/−41	0/0
21	acenaphthene + $C_2H_3^\bullet$ → INT(R4)$^\bullet$ + C_2H_4	0/0	0/0	0/22	−11/−19	0/0
22	INT(R4)$^\bullet$ → acenaphthylene + H$^\bullet$	0/0	−1/0	0/83	−96/−75	−1/0
24	naphthyl$^\bullet$ + C_2H_2 → INT(R5)$^\bullet$	0/6	0/4	0/9	−3 / −22	0/12
26	INT(R5)$^\bullet$ → INT(R6)$^\bullet$	0/6	0/4	0/9	−3 / −22	0/12
27	INT(R6)$^\bullet$ → acenaphthylene + H$^\bullet$	0/6	0/4	0/9	−3 / −22	0/12

[a] Left numbers correspond to 950 K, and right numbers correspond to 1175 K.

TABLE 5: Sensitivity Factors in Percent (γ) for a Factor of 3 Variation in the Rate Constants[a]

no.	reactions	vinylnaphthalene	naphthalene	acenaphthene	acenaphthylene	naphthyl$^\bullet$
1	iodonaphthalene → naphthyl$^\bullet$ + I$^\bullet$	129/25	121 /32	125/21	437/32	108/−5
3	C_2H_4 + H$^\bullet$ $C_2H_3^\bullet$ + H_2	−19/−24	−24/−30	−18/−15	−26/−13	−23/−24
7	iodonaphthalene + H$^\bullet$ → naphthyl$^\bullet$ + HI	131/29	46/13	132/31	115/15	137/−9
8	iodonaphthalene + H$^\bullet$ → naphthalene + I$^\bullet$	−29/0	35/16	−28/8	−60/−16	−33/−2
10	$C_2H_3^\bullet$ + I$^\bullet$ → C_2H_3I	0/7	−1/−3	0/21	−2/−13	−3/12
11	naphthalene → naphthyl$^\bullet$ + H$^\bullet$	−3/−4	0/16	−3/6	−8/−26	−4/−3
12	naphthyl$^\bullet$ + C_2H_4 → INT(R1)$^\bullet$	1/2	−3/−2	1/1	1 /1	−11/−3
13	INT(R1)$^\bullet$ → vinylnaphthalene + H$^\bullet$	149/84	−4/−13	−16/−22	−15/−19	−13/−15
14	INT(R1)$^\bullet$ → INT(R2)$^\bullet$	−46/−31	−13/−18	10/34	10/31	−37/−28
15	INT(R2)$^\bullet$ → acenaphthene + H$^\bullet$	−12/−7	−3/−4	2/8	2/7	−9/−6
16	naphthyl$^\bullet$ + C_2H_4 → naphthalene + $C_2H_3^\bullet$	−12/ −29	57/49	−12/−30	−11/−24	−12/−28
20	acenaphthene + H$^\bullet$ → INT(R4)$^\bullet$ + H_2	0/0	0/0	−2/−44	162/37	0/0
21	acenaphthene + $C_2H_3^\bullet$ → INT(R4)$^\bullet$ + C_2H_4	0/0	0/0	0/−30	21/25	0/0
24	naphthyl$^\bullet$ + C_2H_2 → INT(R5)$^\bullet$	0/−5	0/−3	0/−7	5/18	0/−10

[a] $\gamma = \partial\,[\text{prod}]_i/\partial\,k_j$. Left numbers correspond to 950 K, and right numbers correspond to 1175 K.

iodonaphthalene has already been decomposed. There are however some exceptions. Reaction 16, for example, has an inhibiting effect owing to the turning of active naphthyl radicals to naphthalene. Except for naphthalene the sensitivity factors of the other three major products are negative and increase with temperature since a higher fraction of the radicals react and disappear at the high temperatures.

VII. Conclusions

Iodonaphthalene provides a very useful tool for the production of naphthyl radicals at rather low reflected shock temperatures. With a [ethylene]/[1-iodonaphthalene] ratio of ~100, the reactions of naphthyl radicals are channeled to ethylene rather then to reactions with iodonaphthalene. Also, at the low temperatures used in this investigation the self-dissociation of ethylene is very slow and does not affect the overall kinetics. Two chemical thermometers were used to calculate the reflected shock temperatures.

Four major products—acenaphthene, vinyl naphthalene, naphthalene, and acenaphthylene—were produced upon shock heating and were analyzed by gas chromatography and their yields in terms of mole percent as a function of temperature were calculated. Naphthyl acetylene was not observed experimentally and its calculated yield is by several orders of magnitudes below the yields of the other products. The isomerization reaction acenaphthylene → naphthyl acetylene cannot take place owing to the much higher stability of acenaphthylene[32] relative to that of naphthyl acetylene.

Quantum chemical calculations using uCCSD(T)//uB3LYP/cc-pVDZ level of theory were carried out to evaluate three potential energy surfaces that describe the production of acenaphthene, vinyl naphthalene and acenaphthylene. Rate constants of the elementary steps on the surfaces including their back reactions were calculated using transition state theory.

A kinetics scheme was constructed including the calculated rate constants (and some additional ones) and computer modeling was performed. An excellent agreement between the measured and the calculated yields was obtained.

Acknowledgment. This research was supported by Grant No. 34/01-12.5 from the ISF, The Israel Science Foundation.

References and Notes

(1) Richter, H.; Mazyar, O. A.; Sumathi, R.; Green, W. H.; Howard, J. B.; Bozzelli, J. W. *J. Phys. Chem. A* **2001**, *105*, 1561.
(2) Wang, H.; Frenklach, M. *J. Phys. Chem.* **1994**, 98 11465.
(3) Cioslowski, J.; Piskorz, P.; Moncrieff, D. *J. Org. Chem.* **1998**, *63*, 4051.
(4) Violi, A.; Sarofim, A. F.; Truong, T. N. *Combust. Flame* **2001**, *126*, 1506.
(5) Tokmakov, I. V.; Lin, M. C. *J. Am. Chem. Soc.* **2003**, *125*, 11397.
(6) Bockhorn, H.; Fetting, F.; Wenz, H. W. *Ber. Bunsen-Ges. Phys. Chem.* **1983**, *87*, 1067.
(7) Frenklach, M.; Clary, D. W.; Gardiner, W. C.; Stein, S. E. *Proc. Combust. Inst.* **1984**, *20*, 887.
(8) Frenklach, M.; Warnatz, J. *Combust. Sci. Technol.* **1987**, *51*, 265.
(9) Tokmakov, I. V.; Lin, M. C. *J.Phys. Chem. A,* **2004**, *108*, 9697.
(10) Fahr, A.; Mallard, W. G.; Stein, S. E. *Proc. Combust. Inst.* **1986**, *21*, 825.

(11) Fahr, A.; Stein, S. E. *Proc. Combust. Inst.* **1988**, *22*, 1023.
(12) Yu, T.; Lin. M. C. *Combust. Flame* **1995**, *100*, 169.
(13) Lifshitz, A.; Shweky, I.; Kiefer, J. H.; Sidhu, S. S. In *Shock Waves*; Proceedings of the 18th International Symposium on Shock Waves, Sendia, Japan, 1991; Takayama, K., Ed.; Springer-Verlag: Berlin, 1992; p 825.
(14) Westly, F.; Herron, J. T.; Cvetanovic, R. J.; Hampson, R. F.; Mallard, W. G. *NIST-Chemical Kinetics Standard Reference Database17*, version 5.0; NIST: Washington, DC, 1998 (Best fit).
(15) Stein, S. E.; Lias, S.G.; Liebman, J. F.; Levin, R.D.; Kafafi, S.A. *NIST Standard ReferenceDatabase25*, version 2.0; NIST: Gaithersburg, MD, 1994.
(16) Becke, A. D. *J. Chem. Phys.* **1993**, *98*, 5648.
(17) Lee, C.; Yang, W.; Parr, R. G. *Phys. Rev.* **1988**, *B37*, 785.
(18) Dunning, T. H., Jr. *J. Chem. Phys.* **1989**, *90*, 1007.
(19) Peng, C.; Schlegel, H. B. *Israel J. Chem.* **1993**, *33*, 449.
(20) Pople, J. A.; Head-Gordon, M.; Raghavachari, K. J. *J. Chem. Phys*, **1987**, *87*, 5968.
(21) Frisch, M. J.; Trucks, G. W.; Schlegel, H. B.; Scuseria, G. E.; Robb, M. A.; Cheeseman, J. R.; Montgomery, J. A., Jr.; Vreven, T.; Kudin, K. N.; Burant, J. C.; Millam, J. M.; Iyengar, S. S.; Tomasi, J.; Barone, V.; Mennucci, B.; Cossi, M.; Scalmani, G.; Rega, N.; Petersson, G. A.; Nakatsuji, H.; Hada, M.; Ehara, M.; Toyota, K.; Fukuda, R.; Hasegawa, J.; Ishida, M.; Nakajima, T.; Honda, Y.; Kitao, O.; Nakai, H.; Klene, M.; Li, X.; Knox, J. E.; Hratchian, H. P.; Cross, J. B.; Bakken, V.; Adamo, C.; Jaramillo, J.; Gomperts, R.; Stratmann, R. E.; Yazyev, O.; Austin, A. J.; Cammi, R.; Pomelli, C.; Ochterski, J. W.; Ayala, P. Y.; Morokuma, K.; Voth, G. A.; Salvador, P.; Dannenberg, J. J.; Zakrzewski, V. G.; Dapprich, S.; Daniels, A. D.; Strain, M. C.; Farkas, O.; Malick, D. K.; Rabuck, A. D.; Raghavachari, K.; Foresman, J. B.; Ortiz, J. V.; Cui, Q.; Baboul, A. G.; Clifford, S.; Cioslowski, J.; Stefanov, B. B.; Liu, G.; Liashenko, A.; Piskorz, P.; Komaromi, I.; Martin, R. L.; Fox, D. J.; Keith, T.; Al-Laham, M. A.; Peng, C. Y.; Nanayakkara, A.; Challacombe, M.; Gill, P. M. W.; Johnson, B.; Chen, W.; Wong, M. W.; Gonzalez, C.; Pople, J. A. *Gaussian 03*, revision C.02; Gaussian, Inc.: Wallingford, CT, 2004.
(22) Eyring, H. *J. Chem Phys*, **1935**, *3*, 107.
(23) Evans, M. G.; Polanyi, M. *Trans. Faraday Soc.* **1935**, *31*, 875.
(24) Wigner, E. *Z. Phys. Chem.* **1932**, *B19*, 203.
(25) Louis, F.; Gonzales, C. A.; Huie, R.; Kurylo, M. J. *J. Phys. Chem. A* **2000**, *104*, 8773.
(26) George, P.; Glusker, J. P.; Bock, W. *J. Phys. Chem. A* **2000**, *104*, 11347.
(27) Robaugh, D.; Tsang, W. *J. Phys. Chem.* **1986**, *90*, 5363.
(28) Tsang, W.; Hampson, R. F.; *J. Phys. Chem. Ref. Data* **1986**, *15*, 1087.
(29) Baulch, D.L.; Duxbury, J.; Grant, S.J.; Montague, D.C. *J. Phys. Chem. Ref. Data* **1981**, *10*, Suppl.
(30) Hsu, D. S. Y.; Lin, C. Y.; Lin, M. C. *Proc. Combust. Inst.* **1985**, *20*, 623.
(31) Lifshitz, A.; Tamburu, C.; Dubnikova, F. Unpublished results.
(32) Lifshitz, A.; Tamburu, C.; Dubnikova, F. *Proc. Combust. Inst.* **2007**, *31*, 241.